Real-time Vital Signs Monitoring Based on COTS WiFi Devices

Yu Gu
School of Computer and Information
Hefei University of Technology
Hefei, China
yugu.bruce@ieee.org

Xiang Zhang
School of Computer and Information
Hefei University of Technology
Hefei, China
zhangxiang@mail.hfut.edu.cn

Huan Yan
School of Computer and Information
Hefei University of Technology
Hefei, China
yanhuan@mail.hfut.edu.cn

Zhi Liu
Dept. of Computer and Network Engineering
The University of Electro-Communications
Tokyo, Japan
liu@ieee.org

Yusheng Ji
Information Systems Architecture Science Research Division
National Institute of Informatics
Tokyo, Japan
kei@nii.ac.jp

2021 IEEE International Conference on Bioinformatics and Biomedicine (BIBM) | 978-1-6654-0126-5/21/$31.00 ©2021 IEEE | DOI: 10.1109/BIBM52615.2021.9669403

***Abstract*—Real-time vital signs (breathing and heartbeat) monitoring is essential for patient care and sleep disease prevention. Current solutions are mostly based on wearable sensors or cameras, the former affects the quality of sleep, while the latter is not conducive to privacy protection, and the cost of these methods is usually expensive. In this paper, we propose Wital, a real-time vital signs monitoring system based on the low-cost and widespread COTS WiFi device. Most of the existing WiFi-based vital signs monitoring solutions utilize the line of sight (LOS) WiFi signals to achieve powerful performance. However, in our daily environments, NLOS sensing is more common. In this article, we first model the relationship between the energy ratio of LOS/NLOS signals and the ability to monitor vital signs based on the Ricean-K theory and theoretically prove that blocking LOS signals in NLOS sensing is more beneficial. We have also established a real-time vital signs monitoring system to verify our method, and the experimental results prove the effectiveness of our method.**

***Index Terms*—Wi-Fi, vital Signs, Wireless Sensing**

I. Introduction

Real-time vital signs (breathing and heartbeat) monitoring is essential for patient care and sleep disease prevention. In many examples of sleep disorders, patients only develop symptoms for a short period of time or occasionally, and long-term continuous monitoring is required to detect such symptoms. However, under the condition of limited medical resources caused by Covid-19 and limited funds, long-term hospital observation is unrealistic for most people. Therefore, continuous, real-time and cost-effective vital signs monitoring in the home environment is essential.

Traditional vital signs monitoring schemes mainly leverage attached sensors, such as Polysomnography (PSG) [1] and Electrocardiogram (ECG) [2]. However, these kinds of devices are not suitable for our daily environment, they are expensive and impair the quality of sleep. Solutions based on pressure or acceleration sensors also need to be in contact with the body, and camera based solutions are limited by lighting conditions. Recently, Radio Frequency (RF) based methods [3] has attracted more and more attention as they provided contact-free vital signs monitoring. However, the devices used in these solutions are generally expensive and have disadvantages such as infringement of privacy and discomfort to the wearer.

Recently, COTS WiFi-based vital signs monitoring has received widespread attention [4] due to the widespread and low cost of WiFi devices. The reason why WiFi can detect vital signs is that breathing and heartbeat can cause deformations in the abdomen and chest, and these deformations can affect the propagation of WiFi signals, which can be recorded by the WiFi Channel State Information.

A major challenge for Wi-Fi-based vital signs perception is that the torso deformation caused by breathing/heartbeat is extremely weak, and it is difficult to greatly affect the propagation of Wi-Fi signals. Therefore, a model is needed to guide the system implementation. Currently, state-of-the-art schemes mostly based on the Fresnel Zone model [4] or CSI-ratio model [5] to guide the WiFi-based vital signs monitoring. For the former, the Fresnel Zone model points out that the best performance can be achieved in the case of LOS or close to LOS, however, it is almost impossible to achieve in a real-life environment. For the latter, at least two antennas placed close together are required at the receiver, this is unfavorable for the single-antenna receiver and increases the calculation loss.

In this paper, we propose Wital, a real-time vital signs monitoring system based on low-cost and widespread COTS WiFi devices. To address the aforementioned challenges, we first propose a Ricean-K theory-based model to analyze the relationship between the energy ratio of LOS/NLOS signals and the ability to monitor vital signs, and based on the model analysis, we block the LOS signal to improve the NLOS sensing ability. We also propose a regularity-based motion segmentation algorithm to accurately separate breathing/heartbeat

Corresponding Author: Xiang Zhang
The work was supported in part by ROIS NII Open Collaborative Research 2021(21FA02).

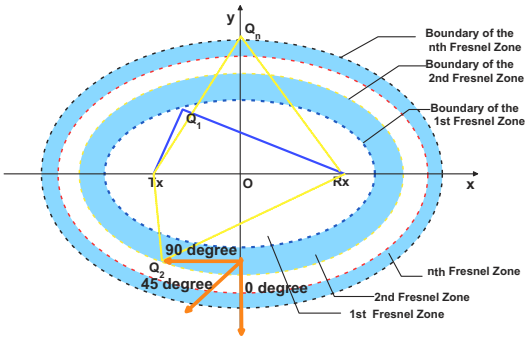

Fig. 1: Fresnel Zone

and other motions.

The main contributions of this paper are summarized as follows:

1) We propose a NLOS sensing model to analyze the relationship between the energy ratio of LOS/NLOS signals and the ability to monitor vital signs.
2) We implement a real-time system using Matlab to evaluate our method. The experimental results indicated the performance of our method.

II. Preliminaries

A. Channel State Information

CSI describes the signal's attenuation on its propagation paths, such as scattering, multi-path fading or shadowing fading caused by motions, and power decay over distance. In the frequency domain, it can be characterized as:

$$Y = H \cdot X + N \tag{1}$$

Where Y and X are the received and transmitted signal vectors, respectively. N is the noise, and H is the CSI channel matrix.

For WiFi CSI, The received signal has a time-varying amplitude in complex plane [6]:

$$|H(f,\theta)|^2 = |H_s(f)|^2 + |H_d(f)|^2 + 2|H_s(f)||H_d(f)|cos\theta \tag{2}$$

θ is the phase difference between the static vector and the dynamic vector, the part that causes the amplitude fluctuation of the CSI waveform is $2|H_s(f)||H_d(f)|cos\theta$. In the case where the range and position of the motion are constant, θ is constant, and the factor affecting the fluctuation range is $|H_s(f)|$ and $|H_d(f)|$.

B. NLOS Sensing Model Based On Ricean-K

In this section, we propose our NLOS sensing model to analyze the relationship between the power ratio of LOS/NLOS signals and the NLOS sensing ability based on the Ricean-K factor.

The Ricean K factor is defined as the ratio of the power in the LOS path to the power in the NLOS path. The baseband in-phase/quadrature-phase (I/Q) representation of the received signal can be expressed as follows [7]:

$$x(t) = \sqrt{\frac{K\Omega}{K+1}} e^{j(2\Pi f_D cos(\theta_0)t)+\phi_0} + \sqrt{\frac{\Omega}{K+1}} h(t) \tag{3}$$

Here K is the Ricean factor, Ω denotes the total received power, θ_0 and ϕ_0 are the Angle of Arrival (AOA) and phase of the LOS, respectively, f_D is the maximum Doppler frequency and $h(t)$ is the diffuse component given by the sum of a large number of multipath components, constituting a complex Gaussian process.

Since antenna do not move in the experiments, ie $f_D = 0$, we simplify Equation (3) to get:

$$x(t) = \sqrt{\frac{K\Omega}{K+1}} e^{\phi_0} + \sqrt{\frac{\Omega}{K+1}} h(t) \tag{4}$$

In the case where the torso does not block LOS, all LOS components and part of NLOS components belong to the static path; part of NLOS components belong to the dynamic path. Combined with Equation (4) and ignoring the transmitted power, we define $|H_s|$ and $|H_d|$ as follows:

$$|H_s| = \frac{K}{K+1} + \frac{1}{K+1} \cdot \rho \tag{5}$$

$$|H_d| = \frac{1}{K+1} \cdot (1-\rho) \tag{6}$$

ρ is the proportion of static paths in the NLOS components. Combine with Equation (2) to get the following equation:

$$\begin{aligned} |H|^2 &= |H_s|^2 + |H_d|^2 + 2|H_s||H_d|cos\theta \\ &= \frac{(K+\rho)^2}{(K+1)^2} + \frac{(1-\rho)^2}{(K+1)^2} \\ &\quad + \frac{2(K+\rho)(1-\rho)}{(K+1)^2} cos\theta \end{aligned} \tag{7}$$

Signal amplitude variation caused by motion can be quantified as:

$$f(K,\rho) = 2|H_s||H_d|cos\theta = \frac{2(K+\rho)(1-\rho)}{(K+1)^2} cos\theta \tag{8}$$

The value of the above formula is related to three variables, namely θ, K and ρ. Consider that the change in phase difference caused by breathing is relatively stable, we omit θ without considering. Then take the derivative of equation 8 of K to get the following formula:

$$f'(K) = \frac{2(1-\rho)(-K^2 - 2\rho K + 1 - 2\rho)}{(K+1)^4} \tag{9}$$

When $K > 1 - 2\rho$, $f(K,\rho)$ decreases as K increases, under normal circumstances, only a small part of the signal of the omnidirectional antenna can be reflected by the human body, which means that ρ is generally bigger than 0.5. In other words, blocking the LOS path appropriately can make CSI more sensitive to motions.

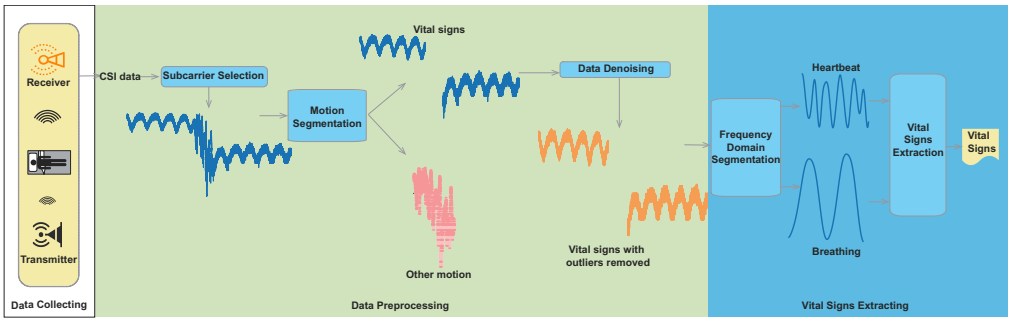

Fig. 2: System architecture

III. System Design

A. System Overview

In this section, we introduce the system design of our real-time vital signs monitoring system, Wital. Our Wital system is shown in Fig. 2, and the system is divided into three modules:
Data Collecting. We collect better CSI data for vital signs monitoring based on our NLOS sensing model (block the LOS).
Data Preprocessing. We select the best performing subcarrier by subcarrier selecting first, then segment the vital signs and other motions based on our motion segmentation algorithm, finally, we denoise the CSI data to remove outliers.
Vital Signs Extracting. Data after preprocessing are divided into two parts by frequency domain segmenting, one mainly including breathing and another one mainly containing heartbeat, then we extract the breathing rate and heart rate, respectively.

B. Data Preprocessing

Subcarrier Selection. According to the previous study [8], for CSI-based sensing, different CSI subcarriers can have different perceived performances even for the same action. Thus, in our system, we first choose a subcarrier that can better capture actions, and we choose the CSI subcarrier with biggest variance for our Wital system.
Data Denoising. Since the collected CSI data contains various environmental noises, in order to obtain a better monitoring effect, we must first reduce the noise of the collected data. In the preprocessing module, we choose the Hampel filter to filter out the outliers which have significantly different values from other neighboring CSI measurements. The goal of the Hampel filter is to identify and replace outliers in a given series. Specifically, we calculate the median of the set consisting of the current CSI sample and its surrounding six samples (three on each side), and use the median absolute deviation to calculate the standard deviation of the set. If the difference between the sample and the median exceeds three times the standard deviation, replace it with the median.

C. Vital Signs Extracting

Frequency Domain Segmentation. The trunk deformation caused by the heartbeat is very small, and the CSI change caused by it can be overwhelmed by the change caused by breathing [9]. Therefore, we need to segment them in the frequency domain first, and in this paper, we segment the CSI based on Butterworth bandpass filters and some prior knowledge in the frequency domain (the frequency range related to the normal heartbeat is 60bpm to 120bpm which corresponds to 1Hz to 2Hz, the frequency range related to normal breathing is 15bpm to 30bpm which corresponds to 0.25Hz to 0.5Hz).
Vital Signs Extracting. After segment the CSI in the frequency domain, we extract the heart and breathing rate by Fast Fourier Transform (FFT). We have also implemented a real-time processing system use Matlab as shown in Figure. 3.

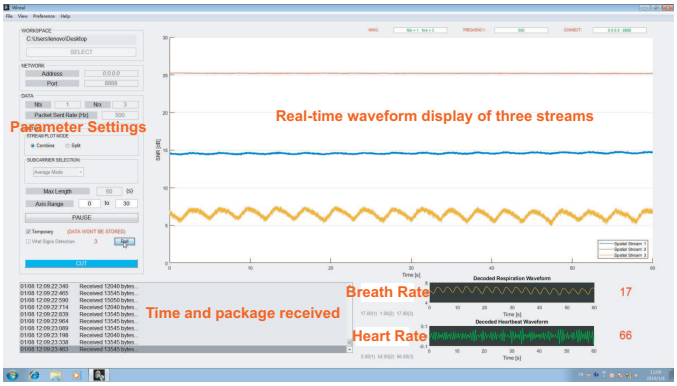

Fig. 3: Real time system's interface.

IV. Experimental Evaluation And Analysis

In this part, we first verify the effectiveness of our NLOS sensing model, then evaluate the proposed real-time vital signs monitoring system-Wital.

A. Evaluation of The NLOS Sensing Model

To verify the proposed NLSO sensing model in section II, we first calculated the Ricean-K value of each stream in one experiment (the setting as shown in Figure.4, and the performance as shown in Figure.5) as shown in Figure. 6, it can be found that the larger the K is, the worse the sensing capability is. Then we placed a lead sheet between the T1-R1 antenna pair in setting 1 (decrease K) to perform a breathing

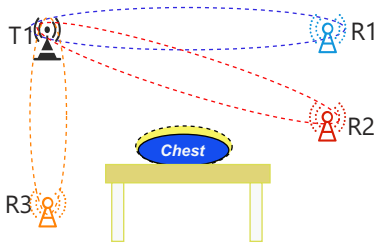

Fig. 4: The antenna settings for the experiments

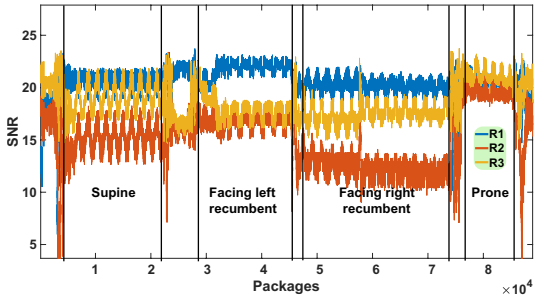

Fig. 5: The performance of breath monitoring

monitoring experiment, the result as shown in Fig.8. It can be found that the motion sensing capability of T1-R1 has been significantly improved. We show the average breathing detection error (BDE), the variance of the CSI waveform (VAR), and the mean amplitude difference (MAD) as Figure.7. We can observe that both the detection accuracy and the sensitivity to motion have improved.

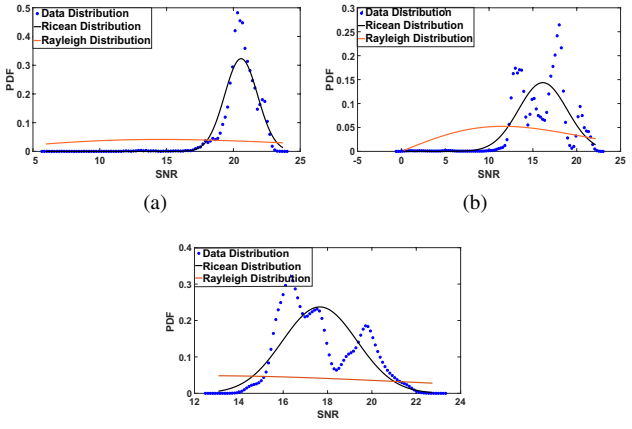

Fig. 6: Distribution of the three streams in Figure.5 (a)T1-R1,K=201.1; (b)T1-R2,K=17.8; (c)T1-R3,K=52.

B. Experimental Setup

In the actual setup, we build our prototype system based on setting as shown in Figure .4 and we choose the T1-R3 stream to obtain vital signs. Based on our NLOS sensing model, we place a lead sheet to block the LOS path of T1-R3.

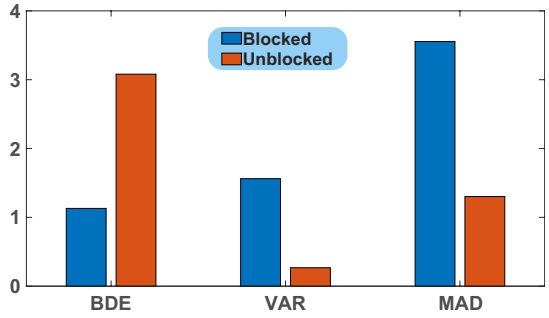

Fig. 7: The average breathing detection error (BDE), the variance of the CSI waveform (VAR), and the mean amplitude difference (MAD) when T1-R1 blocked and unblocked.

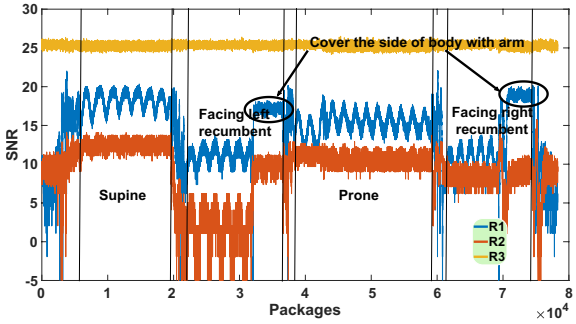

Fig. 8: Obstacle the direct signal from T1 to R1 in setting1, the K factor of the T1-R1 stream decrease to 12.4, the K factor of the T1-R3 stream increase to 5076.

If we choose and block T1-R1, as shown in Figure.8, when the person is facing left/right recumbent, T1-R1 is sensitive to the breath of the mediolateral dimensions. However, when the person's arm blocks the flank, the monitoring effect becomes poor. It is due to when facing left/right recumbent, the main factor that affects the CSI received by R1 is the torso deformation of the flank. This is why we chose T1-R3 to monitor vital signs instead of T1-R1. CSI is collected use csitool [10], and the receiver transmits the received CSI data to the monitor computer for process use our real-time system through the network.

We use COTS devices to implement the proposed system. Specifically, we use two mini PCs with 5300 NIC as the transmitting and the receiving devices, the transmitting device can also be replaced by a WiFi router. The real-time monitoring computer is a desktop computer equipped with an Intel Core i5 3450 CPU (3.1G HZ), 2GB storage.

We experimented in a daily environment as shown in Fig. 9, and ten volunteers participated in our experiments (6 males and 4 females) whose age ranges is 21 to 26, and they are all college students voluntarily participating in the experiment.

Each participant underwent a 30-minute actual test in different natural sleeping positions (prone, supine, left-facing position, and right-facing position). Unlike the previous work [9], we did not control the volunteer's breathing rate, nor did we need to use a directional antenna to monitor the heart rate

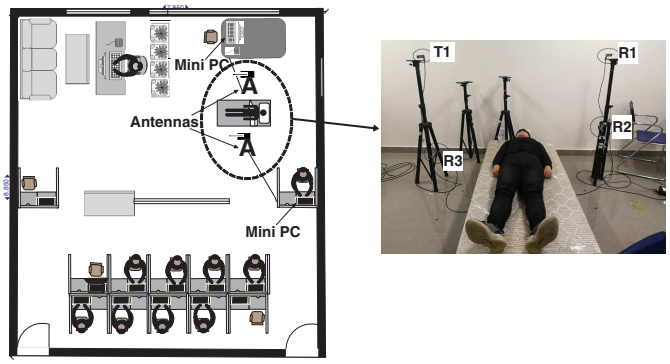

Fig. 9: Prototype System

under LOS conditions. The ground truths of breathing and heartbeat are measured by an accelerometer attached to the abdomen and a fingertip pulse oximeter, respectively.

C. Evaluation Results

Figure. 10 shows the monitored CSI mainly contains the breathing information obtained by the band-pass filter, which is compared with the data of the acceleration sensor attached to the abdomen. We can find that the CSI waveform is highly similar to the data obtained by the acceleration sensor. Figure 11 compares the processed CSI waveform containing the heartbeat with the reading of the accelerometer attached to the chest, we can observe that the occurrence of the heartbeat on the accelerometer is also high consistent with the CSI. These indicate that the CSI obtained from the WiFi signal can be used to extract fine-grained heartbeat and breathing information.

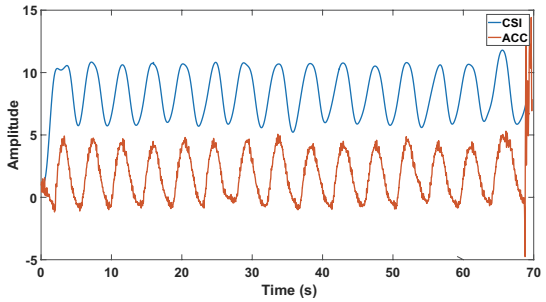

Fig. 10: Comparison of processed CSI and accelerometer (ACC) readings for breathing.

We evaluate the performance of our Wital system under different sleeping positions, and the final result is that the average error of detecting the breathing rate is 0.498 bpm (beats per minute), the average error of detecting the heart rate is 3.531 bpm, and the accuracy is 96.887% and 94.708 %,respectively.

V. Conclusion

In this paer, we propose Wital, a COTS WiFi devices based real-time vital signs monitoring system to track breath and heartbeat with different sleeping postures. To achieve this,

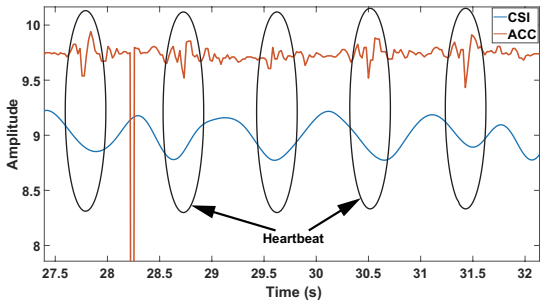

Fig. 11: Comparison of processed CSI and accelerometer (ACC) readings for heartbeat

we propose an NLOS sensing model based on the Ricean-K theory to help monitor the minor displacements caused by vital signs, and we theoretically prove that blocking the LOS signal is more beneficial for motion detection in NLOS sensing. We also implement a real-time prototype system to evaluate our method, and the experimental results indicated the performance of our method.

References

[1] C. A. Kushida, M. R. Littner, T. Morgenthaler, C. A. Alessi, D. Bailey, J. Coleman Jr, L. Friedman, M. Hirshkowitz, S. Kapen, M. Kramer *et al.*, "Practice parameters for the indications for polysomnography and related procedures: an update for 2005," *Sleep*, vol. 28, no. 4, pp. 499–523, 2005.

[2] T. A. Nappholz, W. N. Hursta, A. K. Dawson, and B. M. Steinhaus, "Implantable ambulatory electrocardiogram monitor," May 19 1992, uS Patent 5,113,869.

[3] S. Yue, H. He, H. Wang, H. Rahul, and D. Katabi, "Extracting multi-person respiration from entangled rf signals," *Proceedings of the ACM on Interactive, Mobile, Wearable and Ubiquitous Technologies*, vol. 2, no. 2, pp. 1–22, 2018.

[4] F. Zhang, D. Zhang, J. Xiong, H. Wang, K. Niu, B. Jin, and Y. Wang, "From fresnel diffraction model to fine-grained human respiration sensing with commodity wi-fi devices," *Proceedings of the ACM on Interactive, Mobile, Wearable and Ubiquitous Technologies*, vol. 2, no. 1, p. 53, 2018.

[5] Y. Zeng, D. Wu, J. Xiong, J. Liu, Z. Liu, and D. Zhang, "Multisense: Enabling multi-person respiration sensing with commodity wifi," *Proceedings of the ACM on Interactive, Mobile, Wearable and Ubiquitous Technologies*, vol. 4, no. 3, pp. 1–29, 2020.

[6] H. Wang, D. Zhang, J. Ma, Y. Wang, Y. Wang, D. Wu, T. Gu, and B. Xie, "Human respiration detection with commodity wifi devices: do user location and body orientation matter?" in *Proceedings of the 2016 ACM International Joint Conference on Pervasive and Ubiquitous Computing*. ACM, 2016, pp. 25–36.

[7] C. Tepedelenlioglu, A. Abdi, and G. B. Giannakis, "The ricean k factor: estimation and performance analysis," *IEEE Transactions on Wireless Communications*, vol. 2, no. 4, pp. 799–810, 2003.

[8] Y. Gu, X. Zhang, Z. Liu, and F. Ren, "Wifi-based real-time breathing and heart rate monitoring during sleep," in *2019 IEEE Global Communications Conference (GLOBECOM)*. IEEE, 2019, pp. 1–6.

[9] J. Liu, Y. Chen, Y. Wang, X. Chen, J. Cheng, and J. Yang, "Monitoring vital signs and postures during sleep using wifi signals," *IEEE Internet of Things Journal*, vol. 5, no. 3, pp. 2071–2084, 2018.

[10] D. Halperin, W. Hu, A. Sheth, and D. Wetherall, "Tool release: Gathering 802.11n traces with channel state information," *ACM SIGCOMM CCR*, vol. 41, no. 1, p. 53, Jan. 2011.